Journal of Peptide Science
J. Pept. Sci. 2008; **14**: 76–84
Published online 8 October 2007 in Wiley InterScience (www.interscience.wiley.com). DOI: 10.1002/psc.918

JOURNAL OF PEPTIDE SCIENCE

Conformational studies of vasopressin and mesotocin using NMR spectroscopy and molecular modelling methods. Part I: studies in water

EMILIA SIKORSKA* and SYLWIA RODZIEWICZ-MOTOWIDŁO
Faculty of Chemistry, University of Gdańsk, Sobieskiego 18, 80-952 Gdańsk, Poland

Received 5 June 2007; Accepted 12 July 2007

Abstract: Arginine vasopressin (AVP) and mesotocin (MT) belong to the neurohypophyseal hormone family. The former plays a very important role in the control of urine concentration and the blood pressure in mammals, whereas the latter stimulates uterine concentration and initiates birth in amphibians, marsupials, wallabies, birds, and fishes. Analysis of their 3D structure could be helpful for understanding the evolutionary relationship between all vasopressin- and oxytocin-like hormones. In addition, it allows design of new analogs with appropriate biological activity for humans and animals. In this paper, we present the conformational studies of AVP and MT, under the aqueous conditions. In our investigations, we used 2D NMR spectroscopy and time-averaged molecular dynamics calculations in explicit water. Our studies have shown that both peptides, despite displaying a high sequence homology, differ from each other with regard to the three-dimensional structure. They are in conformational equilibrium as a result of the *cis*/*trans* isomerization across the Cys^6–Pro^7 peptide bond. Both peptides form β-turns in their cyclic part, wherein the *C*-terminal fragment of MT is bent, whereas that of AVP is extended. Copyright © 2007 European Peptide Society and John Wiley & Sons, Ltd.

Keywords: arginine vasopressin (AVP); mesotocin (MT); molecular dynamics; NMR; time-averaged (TAV)

INTRODUCTION

There is a high degree of homology between arginine vasopressin c[Cys^1-Tyr^2-Phe^3-Gln^4-Asn^5-Cys^6]-Pro^7-Arg^8-Gly^9-NH_2 (AVP) and mesotocin c[Cys^1-Tyr^2-Ile^3-Gln^4-Asn^5-Cys^6]-Pro^7-Ile^8-Gly^9-NH_2 (MT), but it is expedient to consider them separately because of their clearly divergent physiological activity, their different gene structure and their different evolutionary lineages. Two evolutionary lineages of neurohypophyseal hormones have been proposed: the isotocin–mesotocin–oxytocin line, associated with reproduction, and the vasotocin–vasopressin line involved in water and electrolyte homeostasis [1]. In the case of evolution line of the AVP, the changes were rather small. The vasotocin, exhibiting both OT and VP activities, has not changed over the last 300 million years, until appearance of the mammals. It is known that isoleucine at position 3 of the OT-like hormones is essential for stimulating OT receptors. Therefore, replacement of Ile^3 with Phe contributed to the loss of the OT activity but procured a strong antidiuretic activity [2]. The VP family hormones contain a basic amino acid (Lys or Arg) at position 8, whereas the OT family contains a neutral hydrophobic amino acid at this position. Arginine or lysine at position 8 of the VP–like hormones is crucial for acting on the VP receptors. Moreover, the difference in the polarity of these amino acid residues is believed to enable the VP and OT peptides to interact with respective receptors.

The evolutionary development of OT-like hormones has mainly run through the substitution at position 4. All mutations resulted from changes in reproductive specialization. Hence, transformation of IT into MT, relying on substitution of Ser^4 with a Gln residue, enhanced contractile activity of the uterine tube, which is very important for oviparous animals.

Even slight changes in the sequence of both hormones trigger considerable differences in their activity. Thus, AVP controls first of all urine concentration [3] and blood pressure [4,5]. Furthermore, it is responsible for stimulation of the adrenocorticotropine secretion [6] and stability of the body temperature [7]. It influences some social, behavioral [8] and sexual reactions [9]. This hormone also causes nonopioid anti-pain effect [10] and drug addiction [11]. It is thought that AVP may influence the higher functions such as memorizing and learning [12]. In turn, MT stimulates uterine contractions and initiates birth. It is crucial for normal birth in the all wallabies [13]. It is possible that MT may be important in male tammars to stimulate contractions of the prostate as well as to influence growth during the breeding season, thereby facilitating ejaculation [14]. The mesotocin is involved in the modulation of the osmotic water permeability in frog urinary bladder [15],

Abbreviations: dDAVP, desmopressin; DSS, 2,2-dimethyl-2-silapentane sulphonic acid; EDMC, electrostatically driven Monte Carlo; RMSD, the root-mean-square deviation; SA, simulated annealing.

*Correspondence to: Emilia Sikorska, Faculty of Chemistry, University of Gdańsk, Sobieskiego 18, 80-952 Gdańsk, Poland;
e-mail: milka@chem.univ.gda.pl

but MT had no effect on the blood pressure in chickens [16] and fishes [17]. In amphibians, the mesotocin has a diuretic effect and acts via the inositol phosphate/calcium signaling pathway. That is completely different from that of AVP, which possesses antidiuretic activity and acts via the adenylate cyclase signaling pathway [18].

Much attention has recently been paid to understanding the relationship between the structure and biological activity. Small peptides, contrary to proteins, display a large conformational freedom. It is supposed that the main structural elements of VP-like hormones are β-turns at positions 3,4 and/or 4,5, whereas β-turns at positions 2,3 and/or 3,4 are characteristic of OT-like peptides [19]. Main conformational properties of VP and OT-like hormones are given in Table 1.

In this paper, we present the conformational analysis of two nonapeptide hormones, AVP and MT, in aqueous environments. In our investigations, we used two-dimensional NMR spectroscopy and molecular dynamics simulation with time-averaged (TAV) NMR restraints including the presence of water molecules.

To date, there has been lack of data concerning conformational properties of MT, except for those using the Raman and the circular dichroism spectroscopies [39]. Therefore, it seems worthwhile to study the structure of this peptide.

We believe that the knowledge of the 3D structure of the peptides can help in understanding evolutionary differences between neurohypophyseal hormones and would contribute to finding structural elements responsible for their biological activities.

MATERIALS AND METHODS

Sample Preparation

The peptides were purchased from Bachem AG. All the peptides were of >95% purity. For samples, 90% H_2O/10% D_2O was used. Samples were made of 5.00 mg and 6.28 mg of AVP and MT, respectively, in 0.6 ml of solvent. The pH of AVP samples in H_2O/D_2O was 5.1 without adjustment. In the case of MT, the pH was adjusted to 2 by using a small volume of a DCl solution. However, earlier CD investigations of the MT showed

Table 1 Conformational characteristics of VP and OT peptides and their representative analogs obtained by experimental methods

	Solvent and methods	Conformational properties	Ref.
VP-like hormones			
AVP	DMSO-d_6, NMR/MD	β 4,5	20
AVP[CH_2]	DMSO-d_6 NMR/MD	Intermediate between types I and II of β-turn at position 3,4	21
dDAVP	H_2O/D_2O (9 : 1), NMR/MD	γ 4	22
	TFE/H_2O (7 : 3), NMR/MD	Short distorted β-sheet with Tyr^2-Phe^3 in the one and Cys^6-Pro^7 linked with Gln^4-Asn^5 β-turn of type I and βII-turn at position 7,8	23
Pressinoic acid	X-ray	β II′ 3,4 and β I 4,5	24
LVP	H_2O/D_2O (9 : 1), NMR/MD	β 3,4	25
[Cpa^1, Sar^7]AVP	DMSO-d_6, NMR/MD	Various types of β-turns at position 3,4	26
Gly-LVP	DMSO-d_6, NMR/MD	An inverse γ-turn at position 4	27
Gly-Gly-Gly-LVP			
desGly^9-AVP	DMSO-d_6, NMR/MD	β 3,4	28
[Acc^2, $DArg^8$]VP	DMSO-d_6, NMR/MD	β IV or II′ 4,5 and βII′ 7,8	29
1-6 the vasopressin-neurophysin	X-ray [1JK4]	βI 3,4 and βI 4,5	30
vasopressin-trypsin complex	X-ray [1YF4]	β 2,3	31
[Sar^7, $MeAla^7$]dAVP	DMSO-d_6, NMR/EDMC	β 4,5	32
OT-like hormones			
OT	DMSO-d_6, NMR/MD	β 3,4	33
dOT	X-ray	βII 3,4 and βI/III 7,8	34,35
[Pen^1]OT	H_2O/D_2O (9 : 1), NMR	γ 2 and γ 4	36
[Pen^1, Leu^2]OT		γ 4	
[dPen^1, Pen^6]OT	H_2O/D_2O (9 : 1), NMR/MD	β 3,4	37
[dPen^1, Pen^6,5-t-$BuPro^7$]OT			
[Mpa^1, c(Glu^4, Lys^8)]OT	DMSO-d_6, NMR/MD	βIII 2,3	38
[dPen^1, c(Gln^4, Lys^8)]OT			

DOI: 10.1002/psc

that the backbone conformation of the peptide is not fundamentally affected by pH changes [39]. Moreover, our investigations (data not shown) indicated that decreasing the pH of aqueous solution caused only slight changes in proton chemical shifts in the direction toward higher values, especially with amide protons. This finding suggests only small changes in the secondary structure of MT to occur upon pH regulation.

NMR Experiments

The NMR spectra were recorded on a 500-MHz Varian spectrometer equipped with a Performa II gradient generator unit, WFG, Ultrashims, high-stability temperature unit and a 5-mm $^{1}H\{^{13}C/^{15}N\}$ PFG triple resonance inverse probe head.

The 2D NMR spectra were measured at 30 °C. The temperature coefficients of the amide proton chemical shifts were measured from 1D NMR spectra for the following temperatures: 2, 10, 20, 30, 40 and 50 °C. Proton resonance assignments were achieved by the use of the proton–proton total chemical shift correlation spectroscopy (TOCSY) [40], the nuclear Overhauser effect spectra (NOESY) [41], the rotating-frame Overhauser enhancement spectroscopy (ROESY) [42,43], as well as the gradient heteronuclear single quantum coherence ($^{1}H-^{13}C$ gHSQC) [44,45] and the gradient heteronuclear multiple quantum coherence ($^{1}H-^{13}C$ gHMBC) techniques [46]. For each sample, the mixing time of 80 ms for TOCSY was measured. The NOESY spectra were recorded with mixing time of 200 ms. The mixing times of the ROESY experiments were set to 200 and 300 ms. The volumes of cross-peaks were picked up for ROESY spectra with a mixing time of 300 ms.

All the spectra were measured with water signal presaturation pulse, typically of 2 dB and 1.5 s. In the case of the 1D NMR spectra, 16 K data points were collected and a spectral width of 6 kHz was used. The 2D homonuclear experiments were measured using a proton spectral width of 4.5 kHz collecting 2K data points.

Vicinal coupling constants, $^{3}J_{NHH\alpha}$, were assigned using ACT-ct-COSY [47] or DQF-COSY [48] for AVP and MT, respectively, and 1D NMR spectra. In ACT-ct-COSY of AVP, the coupling constants were read from the F2 projection and the estimated accuracy of the coupling constants was *ca* 0.1–0.5 Hz. Thus, the DQF-COSY spectrum of MT was processed to enhance the resolution to 1.2 Hz per point in F2. For Gly^{9}, the two $^{3}J_{NHH\alpha}$ coupling constants with H_α protons are equal within the limits of error.

The spectra were calibrated against a HOD signal, taking into account the temperature drift of the reference signal given by the equation $\delta_{1H(T)} = 5.060 - 0.0122T + (2.11 \times 10^{-5})T^2$, [$T$ °C] [49]. External reference signals used for the calibration of the correlation spectra were those of DSS for the carbon axis in the $^{1}H-^{13}C$ spectra ($^{13}C/^{1}H = 0.251449530$) [50].

Spectral processing was carried out using either the NMRPipe/NMRDraw [51] or VNMR [52] and analyzed with XEASY [53].

MD Simulations in Aqueous Solution

Molecular dynamics (MD) simulations were carried out using the AMBER [54] force field. MD calculations were started from random conformations, which were put into water solution. The initial solvent configuration around the peptide was obtained by filling cubic box with water molecules. The overall box size was enlarged by about 8 Å in each direction. A total number of 2469 and 2483 water molecules were used for AVP and MT, respectively. The chloride ions were used to neutralize the system. To equilibrate the solution density, the initial simulations were carried out at 303 K, in a periodic box, until the density was close to 1.0 g/ml. In the next step, the entire system was equilibrated under constant volume per 200 ps.

After equilibration, the MD with TAV distance and dihedral angle restraints derived from the NMR spectroscopy was made. The interproton distances were restrained with the force constants $f = 20$ kcal/(mol × Å^2), and the dihedral angles with $f = 2$ kcal/(mol × rad^2). The improper dihedral angles centered at the C_α atoms were restrained with $f =$ 50 kcal/(mol × rad^2). The geometry of the peptide groups was kept fixed according to the NMR data ($f = 50$ kcal/(mol × rad^2)). The calculations were performed only for major conformations. During MD simulation with TAV, a 8-Å cutoff radius was chosen. The MD simulations were carried out at 303 K in a periodic box of constants volume, with the particle-mesh Ewald (PME) procedure. The time step was 2 fs. The total duration of the run was 4 ns. The coordinates were collected every 2000th step. The conformations obtained during the last 800 ps of simulation were considered in further analysis. As a result, 200 conformations for each peptide were presented.

The interproton distances, used in TAV, were calculated by the CALIBA algorithm of the DYANA [55] program. The macro CALIBA performs calibrations of the cross-peaks using three different calibration classes: cross-peaks assigned to backbone protons (i), cross-peaks assigned to more flexible protons of side chains (ii), and cross-peaks assigned to methyl groups (iii). The calibrations function used for these two classes is: $V = A/d^6$, $V = B/d^4$, and $V = C/d^4$, where V is a peak volume and d is the corresponding distance. We used the value of parameter A corresponding to the intensity of cross-peak between geminal H_β protons (1.8 Å) of Tyr or Phe for each peptide separately [56]. The scalar B was set to $B = A/d_{min}^2$ in order to intersect the backbone calibration curve at d_{min}, and C set to $C = B/3$ (d_{min} – minimal value for distance constraints before possible pseudo atom corrections are added).

The backbone $^{3}J_{NHH\alpha}$ coupling constants were converted to backbone torsion angle ϕ constraints according to the following rules: $^{3}J_{NHH\alpha} < 6$ Hz constrained the ϕ angle to the range of −90° to −30°, 6 Hz $< {}^{3}J_{NHH\alpha} <$ 8 Hz constrained to the range of −120° to −60°, and $^{3}J_{NHH\alpha} > 8$ Hz constrained to the range of −140° to −100° [57].

The results obtained were analyzed using the Carnal and Ptraj programs from the AMBER 8.0 package [54]. Molecular structures were drawn and analyzed with the graphic programs RASMOL [58] and MOLMOL [59].

RESULTS AND DISCUSSION

Analysis of the NMR Spectra

Two distinct sets of proton resonances were found in the NMR spectra of both investigated peptides in aqueous solution. These results indicate that the peptides adopt two conformations being in equilibrium. We suggest that their appearance is due to *cis*/*trans* isomerization of the Cys^{6}–Pro^{7} peptide bond, as reported for AVP by Larive *et al.* [60] but we cannot confirm it by appropriate

DOI: 10.1002/psc

cross-peaks. The contributions of the *cis* isomer are 5 and 6% for AVP and MT, respectively.

The proton and carbon chemical shifts of AVP and MT are given in Tables 2 and 3. The following number of interproton interactions were found in the ROESY spectra: 109 and 102 for AVP and MT, respectively.

Despite the high sequence homology of the presented peptides, the chemical proton shifts differ noticeably from each other, which suggests various three-dimensional structures. However, some similarities are noticed between chemical shifts of the amide protons of the residues at positions 3, 8 and 9.

The presence of all $d_{H\alpha—NH}(i, i+1)$ resonances indicates the *trans* peptide bonds. Both investigated peptides display strong $d_{NH-NH}(5,6)$ and $d_{H\alpha—NH}(4,5)$ ROE effects (Figure 1) enabling to identify the β-turn formation at position 4,5. Additionally, the $d_{H\alpha—NH}(4,6)$ connectivity confirms the β-turn structure in AVP. Moreover, the coupling constants, $^3J_{NHH\alpha}$ for Gln[4] (5.1 Hz and 4.9 Hz for AVP and MT, respectively) and much higher ones for Asn[5] (8.7 Hz and 8.6 Hz for AVP and MT, respectively) confirm the β-turn in the 3–6 fragment. The connectivity $d_{H\alpha—NH}(3,4)$, the $d_{NH-NH}(2,3)$ and the coupling constant for Phe[3] (5.9 and 6.6 Hz for the AVP and the MT, respectively) may indicate the β-turn at position 3,4. In the ROESY spectra of MT, the $d_{NH-NH}(3,4)$ and $d_{NH-NH}(5,6)$ effects may also point to reverse structures in the tocin ring. In turn, the ROE

Table 2 Proton and carbon chemical shifts, the amide proton temperature coefficients, and the vicinal coupling constants of AVP in H_2O/D_2O (9 : 1) solution at 30 °C. Values in brackets belong to the less populated isomer

Residue	Proton and carbon chemical shifts (ppm)						$-\Delta\delta/\Delta T$ (ppb/K)	$^3J_{NHH\alpha}$ (Hz)
	NH	Hα	Hβ	Hγ	Hδ	Others		
Cys[1]		4.20	3.14; 3.35	—	—	—	—	—
		52.55	40.04	—	—	—	—	—
Tyr[2]	8.76	4.56	2.75; 2.83	—	—	$H_{2,6}$6.73;	7.4	7.6
		55.47	36.47	—	—	$H_{3,5}$6.96	—	—
						$C_{2,6}$130.78;		
						$C_{3,5}$115.93		
	(8.73)	(4.55)	(2.71; 2.83)					
Phe[3]	8.02	4.37	2.90; 3.19	—	—	$H_{2,6}$7.13;	8.1	5.9
		55.92	36.54	—	—	$H_{3,5}$7.31;	—	—
						$H_4$7.27		
						$C_{2,6}$129.25;		
						$C_{3,5}$129.11;		
						$C_4$127.46		
	(7.95)	(4.41)	(2.91; 3.21)					
Gln[4]	8.18	4.02	1.94; 1.99	2.19		ε-NH_2 6.76; 7.39	6.8	5.1
		55.15	25.84	31.14	—	—	—	—
	(8.22)	(4.00)	(1.93)	(2.20)				
Asn[5]	8.19	4.69	2.77	—	—	δ-NH_2 6.79; 7.49	6.4	8.7
		50.41	35.90	—	—	—	—	—
	(8.23)	(4.70)	(2.74)					
Cys[6]	8.00	4.81	2.83; 3.09	—	—	—	6.4	7.0
		51.31	38.62	—	—	—		
	(7.77)	(4.45)	(2.90; 3.20)				(6.2)	(7.6)
Pro[7]	—	4.35	1.84; 2.22	1.96	3.64; 3.73	—	—	—
		60.73	29.73	24.72	48.04	—	—	—
	—		(2.09; 2.28)	(1.71; 1.89)	(3.40; 3.54)			
Arg[8]	8.49	4.20	1.70; 1.79	1.58	3.12	ε-NH_2 7.08	9.9	6.5
		53.80	27.98	24.51	40.82			
	(8.43)	(4.22)	(1.73; 1.76)	(1.54)	(3.05)	(ε-NH_2 7.08)	(8.3)	(6.8)
Gly[9]	8.28	3.82	—	—	—	C–NH_2 6.94; 7.34	8.8	5.9
		42.28	—	—	—	—	(8.5)	(6.1)
	(8.36)	(3.82)						

Carbon chemical shifts were found only for more populated isomer.

DOI: 10.1002/psc

Table 3 Proton and carbon chemical shifts, the amide proton temperature coefficients, and the vicinal coupling constants of MT in H_2O/D_2O (9 : 1) solution at 30 °C. Values in brackets belong to the less populated isomer

Residue	Proton and carbon chemical shifts (ppm)						$-\Delta\delta/\Delta T$ (ppb/K)	$^3J_{NHH\alpha}$ (Hz)
	NH	Hα	Hβ	Hγ	Hδ	Others		
Cys[1]	—	4.43	3.45; 3.61	—	—	—	—	—
Tyr[2]	9.11	4.92	3.15; 3.31	—	—	$H_{2,6}$7.36;	6.9	7.8
			38.74	—	—	$H_{3,5}$7.02		
						$C_{2,6}$130.72;		
						$C_{3,5}$115.79		
	(9.16)	(4.94)	(3.15; 3.29)				(8.1)	(8.0)
Ile[3]	8.05	4.19	2.06	1.13; 1.36	1.00		7.7	6.6
		59.73	36.48	24.70	10.53			
	(7.99)	(4.19)	(2.07)				(7.4)	(7.7)
				(1.02)				
Gln[4]	8.34	4.27	2.21	2.54	—	ε-NH_2 7.00;	7.4	4.9
						7.72		
		55.21	26.39	31.50	—		(8.9)	(6.8)
	(8.41)	(4.26)	(2.18)	(2.53)		—		
Asn[5]	8.46	4.88	2.99	—	—	δ-NH_2 7.04;	9.1	8.6
						7.72		
		50.62	36.03	—	—			(7.8)
	(8.60)	(4.76)	(2.97)					
Cys[6]	8.32	5.01	3.11; 3.78	—	—	—	6.0	7.3
			36.46	—	—	—		
	(7.99)	(4.81)	(3.11; 3.26)				(4.4)	(7.3)
Pro[7]	—	4.62	2.07; 2.42	2.17	3.85; 3.90	—	—	—
	—	60.77	29.40	24.74	48.14	—	—	—
			(2.30; 2.50)	(1.96; 2.11)	(3.65; 3.77)			
Ile[8]	8.43	4.27	2.01	1.36; 1.66	1.06	—	8.0	7.2
		59.62	36.13	24.69	10.74			
	(8.51)	(4.23)	(2.61)		(1.09)		(9.4)	(7.8)
				(1.71; 1.39)				
Gly[9]	8.60	4.05	—	—	—	C–NH_2 7.19;	9.7	5.9
						7.54		
		42.28	—	—	—		(9.8)	(6.1)
	(8.67)	(4.05)						

Carbon chemical shifts were only found for more populated isomer.

connectivity $d_{H\alpha—H\beta}(3,6)$ for the MT is characteristic of βIII-turn at position 4,5. The temperature coefficients of all amide protons of the peptides in aqueous solution fall in range $6 \leq -\Delta\delta/\Delta T \leq 10$ ppb/K characteristic of a statistical-coil structure formation. It is possible that in aqueous solution the peptides form open β-turns without intermolecular hydrogen bonds.

The different ROE patterns of two cysteine amino acid residues allow the determination of the geometry of the disulfide bridge [20] for AVP and MT. The $d_{H\beta—H\alpha}(1,6)$ interaction (Figure 1) is characteristic of the positive value of the C_β—S–S–C_β dihedral angle, this corresponding to a right-handed geometry.

Analysis of the Calculated Structures

The structures of the peptides are shown in Figure 2 and are aligned to their first coordinates using Cα atoms from the cyclic part of the molecules. The RMSD values for the ensemble of structures are about 0.1 Å in each case, thus suggesting a very similar structure of the cyclic part of the peptides.

Conformational differences are observed mainly in acyclic parts of the molecules. The analysis of the peptide fluctuations (Figure 3) shows that the positional fluctuations of the Cα atoms of the *C*-terminal fragment of the AVP are larger than those of the MT. In the cyclic regions, the fluctuations do not exceed 0.5 Å.

Results of the calculations reveal that main structural elements of both peptides are β-turns in the cyclic parts. AVP creates two β-turns in the cyclic part of the molecule. Both β-turns (at positions 3,4 and 4,5) are not stabilized by hydrogen bonds. On the basis of the types of β-turns, the conformations of AVP can be divided into two main groups. Both possess a βII-turn at position

DOI: 10.1002/psc

3,4, and in addition, the former creates a βIII′-turn, while the latter type I′ of β-turn at position 4,5.

The analysis of MT structure shows that the type IV of the β-turn at position 3,4 is present. Besides, MT forms an inverse γ-turn with Pro^7 at the top of it, cyclized with a HN^8–CO^6 hydrogen bond. Additionally, the β-turn of type I′ or III′ at position 6,7 was found. MT possesses also βIII-turn in the Cys^6-Gly^9 fragment stabilized by an HN^9–CO^6 hydrogen bond. The appearance of β-turn in the *C*-terminal part of the MT causes the structure to be more compact than in the case of AVP. Moreover, the *C*-terminal amide protons of MT are involved in the hydrogen bond with the carbonyl oxygen atom of Ile^3, which additionally makes the structure more compact.

AVP forms a right-handed disulfide bridge, which is in good agreement with the NMR data and earlier investigations [39]. In turn, MT forms the SS bond with left-handed geometry in aqueous solution. Earlier investigations of the MT [39] revealed the right-handed chirality of the disulfide bridge.

The averaged radius of gyration (*Rg*) calculated for AVP and MT (Table 4) indicate only small differences in size between both peptides within the cyclic part, whereas the acyclic fragment of AVP is much more extended than in MT.

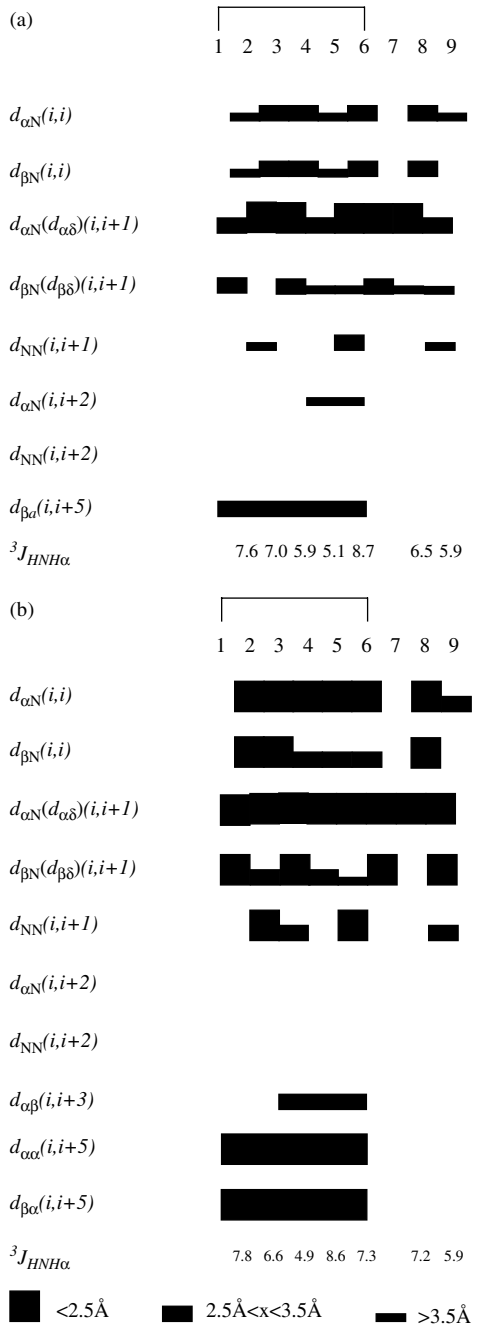

Figure 1 The ROE effects corresponding to their interproton distances and $^3J_{HNH\alpha}$ coupling constants for (a) AVP and (b) MT.

CONCLUSIONS

The results of our investigations show that despite the high sequence homology between AVP and MT, they do differ from each other with regard to the three-dimensional structure. Both possess β-turns in their cyclic part, which is in excellent agreement with earlier investigations of VP- and OT-like peptides. In the case of MT, the *C*-terminal fragment is also involved in type III of β-turn stabilized by the HN^9–CO^6 hydrogen bond. As a result, the *C*-terminal tail of MT is more compact than in AVP. Moreover, a comparison of the *Rg* values of both peptides with the literature data (Table 4) indicates that VP-like hormones are characterized by higher values of *Rg*, especially if the entire molecule is considered. This suggests that the positively charged Arg at position 8 of AVP promotes the extended conformation of the *C*-terminus. These suggestions are well grounded if we take into account the fact that guanidinium of Arg^8 interacts with the extracellular (EL2) loop of the receptor and as a result is exposed to the entrance of the binding pocket [63], which may confirm the extended conformation of the *C*-terminal tail of AVP. Comparison of the AVP and MT structures shows that the replacement of Arg^8 in AVP with Ile^8 in MT changes the conformation in the *C*-terminus and remarkably decreases the flexibility of this fragment. The replacement of Phe^3 in AVP with Ile^3 in MT does not change the secondary structure very markedly, but influences on Tyr^2 side chain orientation. Therefore, the divergence factors by the *C*-terminus, but not in the cyclic part of the neurohormones, could be one of the evolutionary changes responsible for the change of the biological activities from those associated with reproduction (MT) to the activities involved in water and electrolyte homeostasis (AVP).

In conclusion, we have determined the three-dimensional structures of two very important physiological neurohormones, AVP and MT. The analysis of the structural differences induced by the change of

DOI: 10.1002/psc

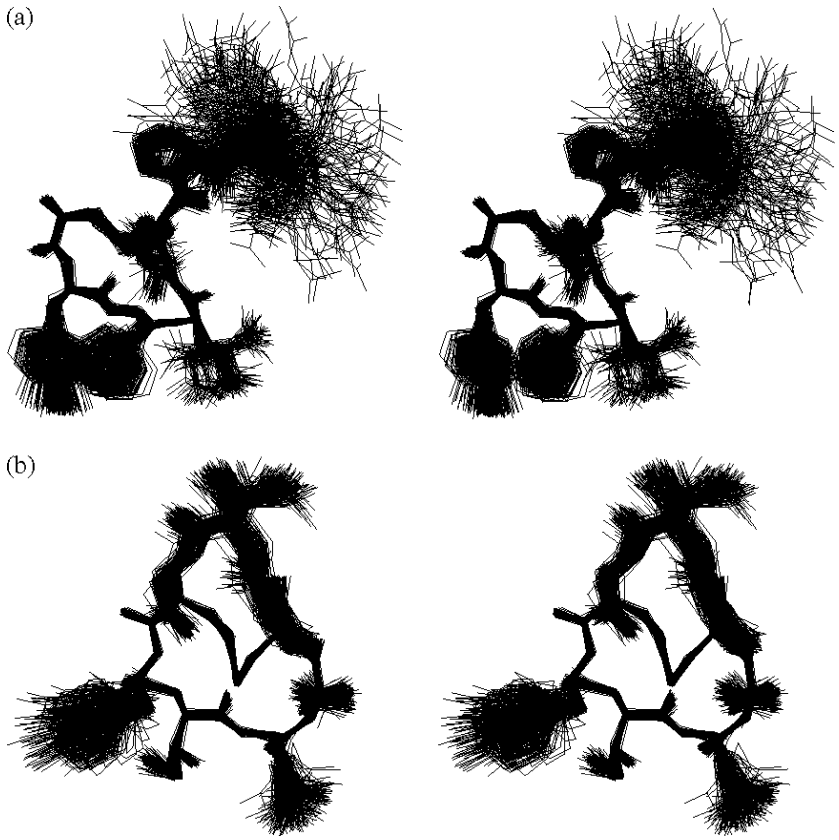

Figure 2 Stereoview of AVP and MT conformations obtained in the last 800 ps of MD simulations with time-averaged distance and dihedral angle restraints, (a) AVP and (b) MT. $RMSD_{1-6} = 0.171$ and 0.108 Å for C_α atoms, respectively.

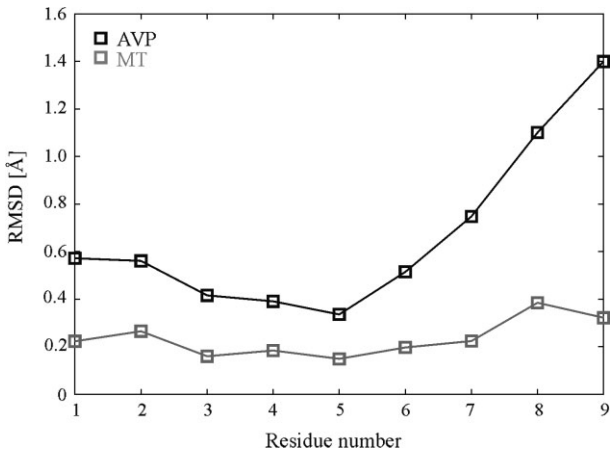

Figure 3 Variation along the polypeptide chain of the time-averaged RMSD fluctuations of the C_α atoms for the AVP and the MT in water.

Table 4 Radius of gyration (*Rg*) calculated for heavy atoms of the peptides and for the VP- and OT-like peptides on the basis of available structures in CSD and PDB data base

Peptide or peptide–protein complex	*Rg* (cyclic part) (Å)		Ref.
AVP in H_2O/D_2O	6.6	4.8	Present study
MT in H_2O/D_2O	5.3	4.8	Present study
1-6 The vasopressin-neurophysin (1JK4)	—	4.9	30
The vasopressin-trypsin (1YF4)	6.4	5.2	31
Pressinoic acid	—	4.6	24
AVP-V_2 receptor	7.3	5.4	61
Deaminooxytocin (1XY2)	5.7	4.8	34
Oxytocin-neurophysin (1NPO)	5.6	4.4	62

The averaged value of *Rg* calculated for the structures obtained in the last 800 ps of molecular dynamics simulations with TAV restraints.

two residues in the sequences gives a basis to understand the mechanism of interactions of VP- and OT-like hormones with their receptors. Moreover, the results should make the design of new analogs with appropriate biological activity easier, both for humans and animals.

Acknowledgements

This work was supported by the Polish Scientific Research Committee Grant KBN 4 T09A 022 22 and DS 8372-4-0138-6 grants. The calculations were carried

DOI: 10.1002/psc

out in the Academic Computer Centre (TASK) in Gdańsk, Poland.

REFERENCES

1. Acher R, Chauvet J, Chauvet MT. Man and the chimaera. Selective versus neutral oxytocin evolution. *Adv. Exp. Med. Biol.* 1995; **395**: 615–627.
2. van Kesteren RE, Smit AB, Dirks RW, De With ND, Geraerts WPM, Joosse J. Evolution of the vasopressin/oxytocin superfamily: characterization of a cDNA encoding a vasopressin-related precursor, preproconopressin, from the mollusc Lymnaea stagnalis. *Proc. Natl. Acad. Sci. U.S.A.* 1992; **89**: 4593–4597.
3. Bockaert J, Roy C, Rajerison R, Jard S. Specific binding of (3H) lysine-vasopressin to pig kidney plasma membranes. Relationship of receptor occupancy to adenylate cyclase activation. *J. Biol. Chem.* 1973; **248**: 5922–5931.
4. Luft FC, Steinberg H, Ganten U, Meyer D, Gless KH, Lang RE, Fineberg NS, Rascher W, Unger T, Ganten D. Effect of sodium chloride and sodium bicarbonate on blood pressure in stroke-prone spontaneously hypertensive rats. *Clin. Sci. (London)* 1988; **74**: 577–585.
5. Versteeg CA, Bohus B, de Jong W. Attenuation by arginine- and desglycinamide-lysine-vasopressin of a centrally evoked pressor response. *J. Auton. Nerv. Syst.* 1982; **6**: 253–262.
6. Jard S, Gaillard RC, Guillon G, Marie J, Schoenenberg P, Muller AF, Manning M, Sawyer WH. Vasopressin antagonists allow demonstration of a novel type of vasopressin receptor in the rat adenohypophysis. *Mol. Pharmacol.* 1986; **30**: 171–177.
7. Wilkinson MF, Kasting NW. The antipyretic effects of centrally administered vasopressin at different ambient temperatures. *Brain Res.* 1987; **415**: 275–280.
8. Wang Z, Young LJ, De Vries GJ, Insel TR. Voles and vasopressin: a review of molecular, cellular, and behavioral studies of pair bonding and paternal behaviors. *Prog. Brain Res.* 1998; **119**: 483–499.
9. Kendrick KM, Keverne EB, Baldwin BA. Intracerebroventricular oxytocin stimulates maternal behaviour in the sheep. *Neuroendocrinology* 1987; **46**: 56–61.
10. Berkowitz BA, Sherman S. Characterization of vasopressin analgesia. *J. Pharmacol. Exp. Ther.* 1982; **220**: 329–334.
11. van Ree JM, De Wied D. Effect of neurohypophyseal hormones on morphine dependence. *Psychoneuroendocrinology* 1977; **2**: 35–41.
12. Barberis C, Tribollet E. The vasopressin and oxytocin receptors in the central nervous system. *Crit. Rev. Neurobiol.* 1996; **10**: 119–154.
13. Siebel AL, Gehring HM, Nave CD, Bathgate RAD, Borchers CE, Parry LJ. Up-regulation of mesotocin receptors in the tammar wallaby myometrium is pregnancy-specific and independent of estrogen. *Biol. Reprod.* 2002; **66**: 1237–1243.
14. Parry LJ, Bathgate RA. Mesotocin receptor gene and protein expression in the prostate gland, but not testis, of the tammar wallaby, Macropus eugenii. *Biol. Reprod.* 1998; **59**: 1101–1107.
15. Shakhmatova EI, Prutskova NP. The role of mesotocin in the regulation of osmotic permeability of the urinary bladder epithelium in the frog. *Ross. Fiziol. Zh. Im. I.M. Sechenova* 1998; **84**: 238–243.
16. Robinzon B, Koike TI, Marks PA. Oxytocin antagonist blocks the vasodepressor but not the vasopressor effect of neurohypophysial peptides in chickens. *Peptides* 1994; **15**: 1407–1413.
17. Le Mevel JC, Pamantung TF, Mabin D, Vaudry H. Effects of central and peripheral administration of arginine vasotocin and related neuropeptides on blood pressure and heart rate in the conscious trout. *Brain Res.* 1993; **610**: 82–89.
18. Kohno S, Kamishima Y, Iguchi T. Molecular cloning of an anuran V(2) type [Arg(8)] vasotocin receptor and mesotocin receptor: functional characterization and tissue expression in the Japanese tree frog (Hyla japonica). *Gen. Comp. Endocrinol.* 2003; **132**: 485–498.
19. Liwo A, Tempczyk A, O3dziej S, Shenderovich MD, Hruby VJ, Talluri S, Ciarkowski J, Kasprzykowski F, Łankiewicz L, Grzonka Z. Exploration of the conformational space of oxytocin and arginine-vasopressin using the electrostatically driven Monte Carlo and molecular dynamics methods. *Biopolymers* 1996; **38**: 157–175.
20. Schmidt JM, Ohlenschläger O, Rüterjans H, Grzonka Z, Kojro E, Pavo I, Fahrenholz F. Conformation of [8-arginine]vasopressin and V1 antagonists in dimethyl sulfoxide solution derived from two-dimensional NMR spectroscopy and molecular dynamics simulation. *Eur. J. Biochem.* 1991; **201**: 355–371.
21. Iwadate M, Nagao E, Williamson MP, Ueki M, Asakura T. Structure determination of [Arg8] vasopressin methylenedithioether in dimethylsulfoxide using NMR. *Eur. J. Biochem.* 2000; **267**: 4504–4510.
22. Walse B, Kihlberg J, Drakenberg T. Conformation of desmopressin, an analogue of the peptide hormone vasopressin, in aqueous solution as determined by NMR spectroscopy. *Eur. J. Biochem.* 1998; **252**: 428–440.
23. Wang J, Hodges RS, Sykes BD. Effect of trifluoroethanol on the solution structure and flexibility of desmopressin: a two-dimensional NMR study. *Int. J. Pept. Protein Res.* 1995; **45**: 471–481.
24. Langs DA, Smith GD, Stezowski JJ, Hughes RE. Structure of pressinoic acid: the cyclic moiety of vasopressin. *Science* 1986; **232**: 1240–1242.
25. Yu C, Yang TH, Yeh CJ, Chuang LC. Combined use of NMR, distance geometry, and restrained energy minimization for the conformational analysis of 8-lysine-the vasopressin. *Can. J. Chem.* 1992; **70**: 1950–1955.
26. Shenderovich MD, Kasprzykowski K, Liwo A, Sekacis IP, Saulitis J, Nikiforovich GV. Conformational analysis of [Cpp^1, Sar^7, Arg^8] the vasopressin by ^{1}H-NMR spectroscopy and molecular mechanics calculations. *Int. J. Pept. Protein Res.* 1991; **38**: 528–538.
27. Zieger G, Andreae F, Sterk H. Assigment of proton NMR resonances and conformational analysis of [Lys^8]-the vasopressin homologues. *Magn. Reson. Chem.* 1991; **29**: 580–586.
28. Shenderovich MD, Sekatsis IP, Liepin'sh EE, Nikoforovich G, Papsuevich OS. Study of the spatial structure of des-Gly^9-[Arg^8] the vasopressin by two-dimensional NMR spectroscopy and theoretical conformation analysis. *Bioorg. Khim.* 1985; **11**: 1180–1191.
29. Sikorska E, Ślusarz R, Lammek B. Conformational studies of highly potent 1-aminocyclohexane-1-carboxylic acid substituted V_2 vasopressin agonists. *J. Pept. Res.* 2005; **66**(Suppl. 1): 30–40.
30. Wu CK, Hu B, Rose JP, Liu ZJ, Nguyen TL, Zheng TL, Breslow E, Wang BC. Structures of an unliganded neurophysin and its the vasopressin complex: implications for binding and allosteric mechanisms. *Protein Sci.* 2001; **10**: 1869–1880.
31. Ibrahim SB, Pattabhi V. Trypsin inhibition by a peptide hormone: crystal structure of trypsin-vasopressin complex. *J. Mol. Biol.* 2005; **348**: 1191–1198.
32. Rodziewicz-Motowid3o S, Zhukov I, Kasprzykowski F, Grzonka Z, Ciarkowski J, Wójcik J. Conformational solution studies of (Sar(7))desamino- and (MeAla(7)) desamino-vasopressin analogues using NMR spectroscopy. *J. Pept. Sci.* 2002; **8**: 347–364.
33. Bhaskaran R, Chuang LC, Yu C. Conformational properties of oxytocin in dimethyl sulfoxide solution – NMR and restrained molecular dynamics studies. *Biopolymers* 1992; **32**: 1599–1608.
34. Wood SP, Tickle IJ, Treharne AM, Pitts JE, Mascarenhas Y, Li JY, Husain J, Cooper S, Blundell TL, Hruby VJ, Buku A, Fischman AJ, Wyssbrod HR. Crystal structure analysis of deamino-oxytocin: conformational flexibility and receptor binding. *Science* 1986; **232**: 633–636.
35. Husain J, Nlundell TL, Cooper S, Pitts JE, Tickle IJ, Wood SP, Hruby VJ, Buku A, Fischman AJ, Wyssbrod HR, Mascerenhas Y. The conformation of deamino-oxytocin: X-ray analysis of the 'dry' and 'wet' forms. *Philos. Trans. R. Soc. Lond., B, Biol. Sci.* 1990; **327**: 625–654.

36. Mosberg HI, Hruby VJ, Meraldi JP. Conformational study of the potent peptide hormone antagonist [1-penicillamine,2-leucine]oxytocin in aqueous solution. *Biochemistry* 1981; **20**: 2822–2828.
37. Bélec L, Blankenship JW, Lubell W. Examination of structural characteristics of the potent oxytocin antagonists (dPen^1, Pen^6)-OT and (dPen^1, Pen^6,5-tBuPro^7)-OT by NMR, Raman, CD spectroscopy and molecular modeling. *J. Pept. Sci.* 2005; **11**: 365–378.
38. Shenderovich MD, Kövér KE, Wilke S, Collins N, Hruby VJ. Solution conformations of potent bicycle antagonists of oxytocin by nuclear magnetic resonance spectroscopy and molecular dynamic simulations. *J. Am. Chem. Soc.* 1997; **119**: 5833–5846.
39. Tu AT, Lee J, Deb KK, Hruby VJ. Laser Raman spectroscopy and circular dichroism studies of the peptide hormones the mesotocin, vasotocin, lysine the vasopressin, and arginine the vasopressin. *J. Biol. Chem.* 1979; **254**: 3272–3278.
40. Bax A, Freeman R. Enhanced NMR resolution by restricting the effective sample volume. *J. Magn. Reson.* 1985; **65**: 355–360.
41. Kumar A, Ernst RR, Wüthrich K. A two-dimensional nuclear Overhauser enhancement (2D NOE) experiment for the elucidation of complete proton-proton cross relaxation networks in biological macromolecules. *Biochem. Biophys. Res. Commun.* 1980; **95**: 1–10.
42. Bothner-By AA, Stephens RL, Lee JM, Warren CD, Jeanloz RW. Structure determination of a tetrasaccharide: Transient nuclear Overhauser effects in the rotating frame. *J. Am. Chem. Soc.* 1980; **106**: 811–813.
43. Bax A, Davis DG. Practical aspects of two-dimensional transverse NOE spectroscopy. *J. Magn. Reson.* 1985; **63**: 207–213.
44. Kay LE, Keifer P, Saarinen T. Pure absorption gradient enhanced heteronuclear single quantum correlation spectroscopy with improved sensitivity. *J. Am. Chem. Soc.* 1992; **114**: 10663–10665.
45. Kontaxis G, Stonehouse J, Laue ED, Keeler J. The sensitivity of experiments which use gradient pulses for coherence-pathway selection. *J. Magn. Reson., Ser. A* 1994; **111**: 70–76.
46. Bax A, Summers MF. Proton and carbon 13 assignments from sensitivity-enhanced detection of heteronuclear multiple-bond connectivity by 2D multiple quantum NMR. *J. Am. Chem. Soc.* 1986; **108**: 2093–2094.
47. Koźmiński W. The new active-coupling-pattern tilting experiment for an efficient and accurate determination of homonuclear coupling constants. *J. Magn. Reson.* 1998; **134**: 189–193.
48. Rance M, Sorenson OW, Bodenhausen G, Wagner G, Ernst RR, Wüthrich K. Improved spectral resolution in cosy ^{1}H NMR spectra of proteins via double quantum filtering. *Biochem. Biophys. Res. Commun.* 1983; **117**: 479–485.
49. Gottlieb HE, Kotlyar V, Nudelman A. NMR chemical shifts of common laboratory solvents as trace impurities. *J. Org. Chem.* 1997; **62**: 7512–7515.
50. Wishart DS, Bigam CG, Holm A, Hodges RS, Sykes BD. ^{1}H, ^{13}C and ^{15}N random coil NMR chemical shifts of the common amino acids. I. Investigations of nearest-neighbor effects. *J. Biomol. NMR* 1995; **5**: 67–81.
51. Delaglio F, Grzesiek S, Geerten WV, Zhu G, Pfeifer J, Bax A. NMRPipe: a multidimensional spectral processing system based on UNIX pipes. *J. Biomol. NMR* 1995; **6**: 277–293.
52. Varian, Nuclear Magnetic resonance Instruments, VnmrTM Software, Revision 5.3B 1/97.
53. Bartles C, Xia T, Billeter M, Günter P, Wütrich K. The program XEASY for the computer-supported NMR spectral analysis of biological macromolecules. *J. Biomol. NMR* 1995; **5**: 1–10.
54. Case DA, Darden TA, Cheatham TE III, Simmerling CL, Wang J, Duke RE, Luo R, Merz KM, Wang B, Pearlman DA, Crowley M, Brozell S, Tsui V, Gohlke H, Mongan J, Hornak V, Cui G, Beroza P, Schafmeister C, Caldwell JW, Ross WS, Kollman PA. *AMBER 8*. University of California: San Francisco, 2004.
55. Güntert P, Mumenthaler C, Wüthrich K. Torsion angle dynamics for NMR structure calculation with the new program DYANA. *J. Mol. Biol.* 1997; **273**: 283–298.
56. Bolton PH, Carlson RMK, Croasmun WR, Crouch RC, Dabrowski J, Dyson HJ, Goljer I, Gray GA, Griesinger C, Hull WH, Kalbitzer HR, Kessler H, Martin GE, Rinaldi PL, Sattler M, Schleucher J, Schwalbe H, Seip S, Wright PE. In *Two-Dimensional NMR Spectroscopy: Applications for Chemists and Biochemists*, Croasmun WR, Carlson RMK (eds.). VCH: New York, 1994 .
57. Pardi A, Billeter M, Wüthrich K. Calibration of the angular-dependence of the amide proton-C-alpha proton coupling-constants, 3JHN alpha, in a globular protein. Use of 3JHN alpha for identification of helical secondary structure. *J. Mol. Biol.* 1984; **180**: 741–751.
58. Sanchez-Ferrer A, Nunez-Delicado E, Bru R. Software for viewing biomolecules in three dimensions on the Internet. *Trends Biochem. Sci.* 1995; **20**: 286–288.
59. Koradi R, Billeter M, Wüthrich K. MOLMOL: a program for display and analysis of macromolecular structures. *J. Mol. Graphics* 1996; **14**: 52–55.
60. Larive CK, Guerra L, Rabenstein DL. Cis/trans conformational equilibrium across the cysteine^6-proline peptide bond of oxytocin, arginine the vasopressin, and lysine the vasopressin. *J. Am. Chem. Soc.* 1992; **114**: 7331–7337.
61. Czaplewski C, Kaźmierkiewicz R, Ciarkowski J. Molecular modeling of the human the vasopressin V2 receptor/agonist complex. *J. Comput. Aided Mol. Des.* 1998; **12**: 275–287.
62. Rose JP, Wu CK, Hsiao CD, Breslow E, Wang BC. Crystal structure of the neurophysin-oxytocin complex. *Nat. Struct. Biol.* 1996; **3**: 163–169.
63. Ślusarz MJ, Giełdoń A, Ślusarz R, Ciarkowski J. Analysis of interactions responsible for vasopressin binding to human neurohypophyseal hormone receptors – molecular dynamics study of the activated receptor–vasopressin–Gα systems. *J. Pept. Sci.* 2006; **12**: 180–189.

DOI: 10.1002/psc